BAMS Article

The Hydrometeorological Observation Network in California's Russian River Watershed

Development, Characteristics, and Key Findings from 1997 to 2019

Edwin Sumargo, Anna M. Wilson, F. Martin Ralph, Rachel Weihs, Allen White, James Jasperse, Maryam Asgari-Lamjiri, Stephen Turnbull, Charles Downer, and Luca Delle Monache

ABSTRACT: The Russian River Hydrometeorological Observing Network (RHONET) is a unique suite of high-resolution in situ and remote sensing observations deployed over 20 years to address both scientific and operational gaps in understanding, monitoring, and predicting weather and water extremes on the United States' West Coast. It was created over many years by diverse organizations ranging from universities to federal, state, and local government agencies and utilities. Today, RHONET is a hybrid network with diverse observation sets aimed at advancing scientific understanding of physical processes driving extreme precipitation and runoff in the region. Its development is described, including the specific goals that led to a series of network enhancements, as well as the key characteristics of its sensors. The hydroclimatology of the Russian River area is described, including an overview of the hydrologic extremes and variability driving the scientific and operational needs in the region, from atmospheric river behavior and orographic precipitation processes to hydrologic conditions related to water supply and flooding. A case study of Lake Mendocino storage response to a landfalling atmospheric river in 2018 is presented to demonstrate the network's performance and hydrologic applications during high-impact weather events. Finally, a synopsis of key scientific findings and applications enabled by the network is provided, from the first documentation of the role of landfalling atmospheric rivers in flooding, to the occurrence of shallow nonbrightband rain, to the buffering influence of extremely dry soils in autumn, and to the development of forecast-informed reservoir operations for Lake Mendocino.

https://doi.org/10.1175/BAMS-D-19-0253.1
Corresponding author: Edwin Sumargo, esumargo@ucsd.edu
In final form 11 May 2020

AFFILIATIONS: Sumargo, Wilson, Ralph, Weihs, Asgari-Lamjiri, and Delle Monache—Center for Western Weather and Water Extremes, Scripps Institution of Oceanography, University of California, San Diego, La Jolla, California; **White**—NOAA/Physical Science Laboratory, Boulder, Colorado; **Jasperse**—Sonoma Water, Santa Rosa, California; **Turnbull and Downer**—U.S. Army Engineer Research and Development Center, Vicksburg, Mississippi

The Russian River Hydrometeorological Observing Network (RHONET) has emerged over 20 years, driven by a series of developments in scientific programs and their application to meet operational challenges. The current network (Fig. 1a), as of 2019, represents a combination of influences originating from an overarching goal to advance scientific understanding of physical processes that create extreme precipitation in the region. The current network design is the result of interagency cooperation (Table 1), including universities and federal, state, and local government agencies. The network's operational aims range from improving precipitation forecasts [partly through the interagency United States Weather Research Program (USWRP); Fritsch and Carbone 2004; Ralph et al. 2005a], to developing new monitoring and forecasting methods and tools [through National Oceanic and Atmospheric Administration's Hydrometeorology Testbed (NOAA HMT) as a part of the California Department of Water Resources' Enhanced Flood Response and Emergency Preparedness program (CADWR EFREP); Ralph and Dettinger 2011], to supporting the development of requirements to restore endangered salmon (through NOAA's Habitat Blueprint program; NOAA 2019b), and most recently to developing new reservoir operations methods that take advantage of improved forecasts of atmospheric rivers (ARs) [through the multiagency Forecast-Informed Reservoir Operations (FIRO) program; Center for Western Weather and Water Extremes (CW3E); CW3E 2017; Jasperse et al. 2017] (Fig. 1b).

The existence of RHONET has attracted major field campaigns that leveraged the infrastructure in place at the time, such as CalWater-1 (2011), CalWater-2 (2014–15), and the Department of Energy's Atmospheric Radiation Measurement Cloud Aerosol Precipitation Experiment (ACAPEX). The evolution of this unique observing network represents the diverse range of challenges and approaches taken in this basin to deal with one of the most variable hydroclimates in the nation (Dettinger et al. 2011), in one of the most populous and productive states. However, there remains a need for comprehensive documentation of the evolution and the current state of this unique observing network, which has benefited hydrometeorological science and operations (Table 1). Thus, the purpose of this paper is to fill this gap by describing the history of hydrometeorological sensor network evolution, the current state of the network, and the research and operational significance of the network.

Although this sensor network evolution historically took place broadly in California, the Russian River basin has been the forefront of this evolution. For this reason, the following sections will focus on the sensor network evolution within and around the Russian River basin, primarily precipitation, soil moisture, and streamflow measurements. Specifically, we will describe the basin geography and hydroclimatology in the second section to contextualize the weather and climatic processes affecting the basin hydrology. We will also describe the four epochs of RHONET evolution and its current state in the third and fourth sections, respectively, as a comprehensive documentation on the development of RHONET, from its conception to the current availability and applications. A short case study involving RHONET

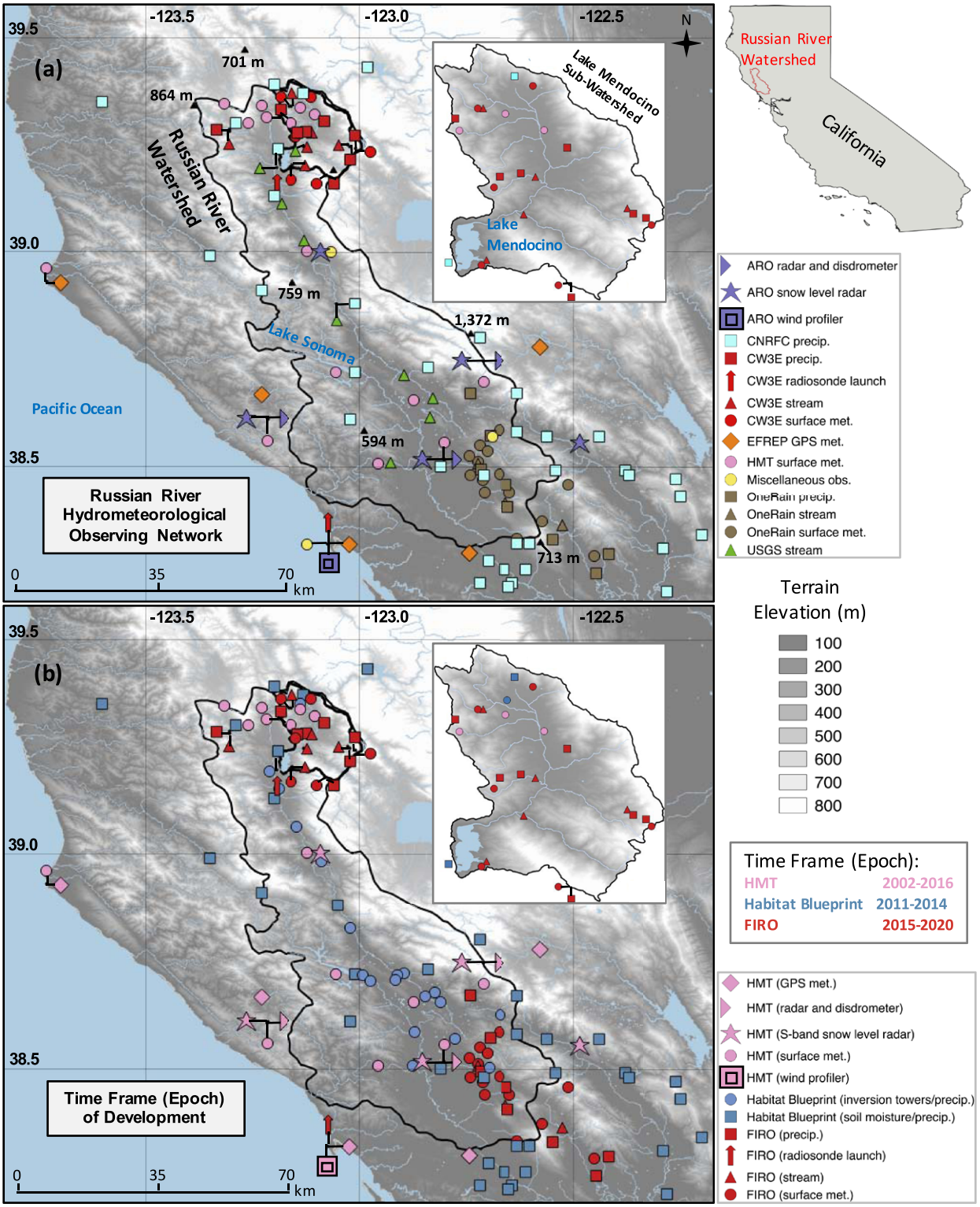

Fig. 1. Terrain base maps showing (a) the existing RHONET in the Russian River watershed and the immediate surrounding areas and (b) its development throughout the HMT, Habitat Blueprint, and FIRO epochs. The thick boundaries demarcate the Lake Mendocino subwatershed. Different colors represent different (a) networks and (b) epochs. The inset maps show those within the Lake Mendocino area. (top right) The California map displays the location of Russian River watershed in California.

will be presented in the fifth section to illustrate the importance of continuous and spatially dense observations for hydrologic analyses and applications. Finally, the relevance to the broader hydrometeorological community and the research and operational benefits will be covered in the sixth and seventh sections, respectively.

Table 1. The timeline of the four epochs associated with hydrometeorological observations in California and examples of key publications emerging from different programs leveraging RHONET during the four epochs.

Epoch	Year																							
	1997	1998	1999	2000	2001	2002	2003	2004	2005	2006	2007	2008	2009	2010	2011	2012	2013	2014	2015	2016	2017	2018	2019	2020
CALJET and PACJET	White et al. (2000, 2002, 2003), Ralph et al. (2003, 2004, 2005b, 2016a), Neiman et al. (2004, 2005, 2006, 2016), Kingsmill et al. (2006)																							
HMT						Ralph et al. (2005b, 2010, 2013a,b, 2016b), Morss and Ralph (2007), Martner et al. (2008), Zamora et al. (2011), Zhang et al. (2012), Kingsmill et al. (2013, 2016), White et al. (2013, 2015), Matrosov et al. (2014), Chen et al. (2019)																	
NOAA Habitat Blueprint															Reynolds et al. (2016)									
FIRO																			Cannon et al. (2017), Jasperse et al. (2017), Lamjiri et al. (2017), Martin et al. (2018, 2019a,b), Ralph et al. (2019a,b)					

Geography and hydroclimatology of the Russian River basin

The Russian River drains an area of 1,485 mi^2 (3,846 km^2) across parts of Sonoma and Mendocino Counties in Northern California (Sonoma Water 2018a). It originates near Redwood Valley and Potter Valley in Mendocino County and drains into the Pacific Ocean at Jenner in Sonoma County. Two major reservoirs reside within the Russian River drainage: Lake Mendocino on the East Fork of Russian River and Lake Sonoma on Dry Creek, both of which serve as flood protection and water supply storage.

Northern California, where the Russian River basin resides, has a Mediterranean climate characterized by warm and dry summers and cool and wet winters, with ~80% of the precipitation occurring between November and March (Flint et al. 2018). The weather in the region is susceptible to incoming Pacific storm systems, owing to its close proximity to the northeast Pacific. Of all storms affecting Northern California, ARs are responsible for the heaviest rainfalls (Ralph et al. 2006, 2013a; Lamjiri et al. 2017) and most of the flood damages (Corringham et al. 2019) in the region, and have increasingly become dominant contributors to California water resources and extremes (Gershunov et al. 2019). Furthermore, the mountainous terrain of the Russian River basin favors orographic precipitation processes (Ralph et al. 2006) and impairs the already-sparse operational radars' coverage of shallow nonbrightband rain that accounts for 12%–15% of the total precipitation (Matrosov et al. 2014). Therefore, in situ monitoring of precipitation and surface and subsurface waters with high spatial and temporal resolution is essential for hydrologic applications in the region.

The basin-mean water year (WY) total precipitation is as low as 623 mm (WY 2014) and as high as 2,097 mm (WY 1983). It averages 1,131 mm over WYs 1982–2018, where wetter years are characterized by more ARs (Dettinger et al. 2011). Figure 2a displays the amounts of WY 2016 total precipitation at grid points of the Parameter-Elevation Regressions on Independent Slopes Model (PRISM; Daly et al. 1994, 2008) within the Russian River basin. WY 2016 was nominally an average precipitation year, where the basin-mean WY total precipitation is closest to the WYs 1982–2018 average. WY total precipitation is typically greater at higher elevations, owing partly to the orographic enhancement. The coefficients of variation of WYs 1982–2018 total precipitation are shown in Fig. 2b to illustrate the magnitudes of interannual variation of annual total precipitation relative to the average. Consistent with Dettinger et al. (2011), the coefficients of variation amount to 0.32–0.38, indicating the high variability of the region's

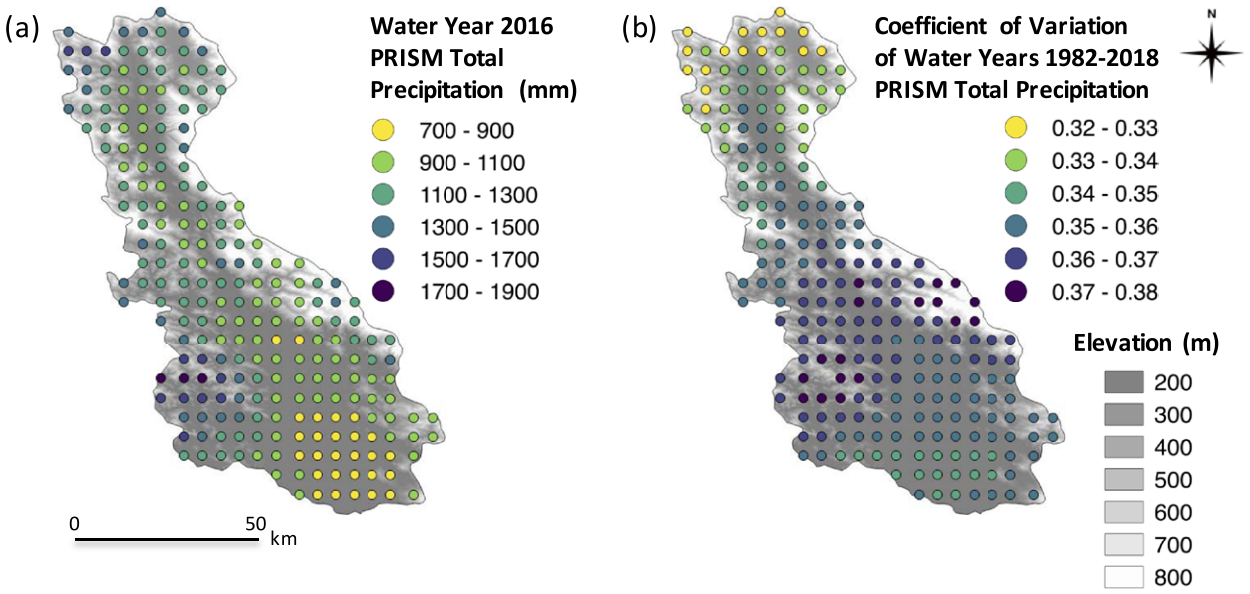

Fig. 2. Terrain base map of Russian River basin, showing (a) the WY 2016 (4 km, daily) PRISM (Daly et al. 1994, 2008) total precipitation and (b) the coefficient of variation (standard deviation divided by mean) of WYs 1982–2018 PRISM total precipitation. The PRISM precipitation dataset is obtained from the PRISM Climate Group (2019).

hydroclimate relative to the rest of the United States, where the coefficients of variation are mostly <0.3. The coefficients of variation also tend to be greater in the southern portion of the basin.

Streamflow time series reveal similar interannual variations. The relatively normal WY 2016, wet WY 2017, and dry WY 2018 illustrate the variations by showing different baseflow and storm runoff magnitudes and frequencies in three different WYs (Fig. 3, left panel). The WY total flow volume records from four U.S. Geological Survey's (USGS's) stream gauges in the Russian River watershed reveal WY 2014 to be the driest and WY 1998 to be the wettest (Fig. 3, right panel). (Note that only WY 1988 onward are considered due to the data availability at Calpella gauge). Averaged over WYs 1988–2018, storm runoff accounts for roughly half of the total flow volumes. The fractions of storm runoff to the total flow are greater downstream, from 0.35 at Calpella near the headwaters to 0.59 at Guerneville near the outlet to Pacific Ocean. The relatively low storm runoff fraction at Calpella, however, to a certain degree reflects the influence of Eel River flow diversion into the Russian River associated with the Potter Valley Project (Potter Valley Project 2020). Likewise, the coefficients of variation of the WY total flow volume span from 0.43 at Calpella to 0.65 at Guerneville. Nevertheless, these numbers capture the upstream-to-downstream streamflow variations and interannual variability, which illustrate the need for long-term continuous monitoring systems with high spatial density.

The epochs of hydrometeorological sensor network evolution in California

The first epoch: CALJET and PACJET. The California Land-Falling Jets Experiment (CALJET; Neiman et al. 2004; Ralph et al. 2003, 2004, 2005a) and Pacific Land-Falling Jets Experiment (PACJET; White et al. 2002; Neiman et al. 2005; Ralph et al. 2005b) were a series of wintertime field campaigns taking place across the West Coast of the United States in 1997–98 and 2000–04, respectively (Neiman et al. 2006; Table 1). Both experiments were early hydrometeorological observation efforts predating the era of automated and real-time observations. This era was marked by sporadic traditional field campaigns, where a team of scientists and engineers were deployed to the field for weeks at a time.

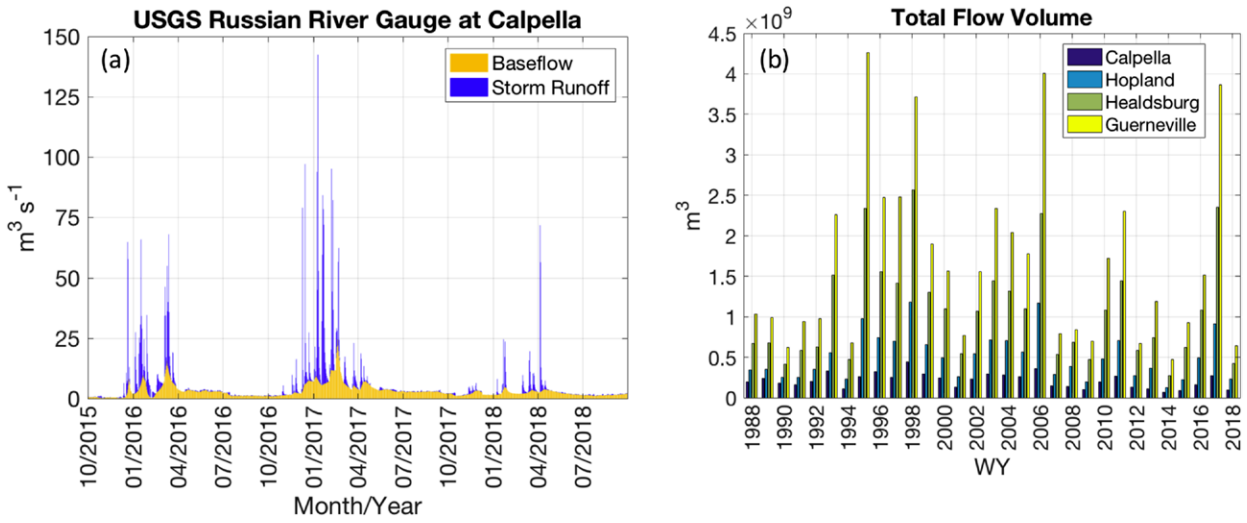

Fig. 3. (a) WYs 2016–18 baseflow and storm runoff time series derived from USGS Russian River stream discharge record at Calpella (gauge 11461500). Baseflow and storm runoff are computed using local minimum method for hydrograph separation based on USGS HYSEP algorithm (Sloto and Crouse 1996). (b) WYs 1988–2018 total flow volumes from USGS Russian River stream gauges at (from upstream to downstream) Calpella, Hopland (11462500), Healdsburg (11464000), and Guerneville (11467000).

The CALJET and PACJET experiments employed NOAA P-3 research aircraft to profile coastal and offshore orographically modulated flows associated with cold fronts and their prefrontal low-level jets during landfalling winter storms (Neiman et al. 2016; Ralph et al. 2016a). The objectives of both experiments were to explore the role of these observations on mesoscale quantitative precipitation and wind forecasting and, in the CALJET experiment, to investigate the influence of the strong 1997/98 El Niño conditions on flood risk in California (Ralph et al. 2016a).

The second epoch: HMT. Researchers later realized the need of improving the frequency and consistency of observations as well as the cost and efficiency of field campaigns (Fritsch and Carbone 2004; Ralph et al. 2005a). The proposed solution was installing and maintaining permanent automated observation stations having the capability of directly reporting to the users via telemetry. The NOAA HMT was the manifestation of this solution, specifically the HMT-West (Ralph et al. 2005a; Morss and Ralph 2007). This effort primarily consisted of two phases occurring in 2002 and 2010 (Table 1). However, the instruments were installed sporadically over the period from 2005 to 2016 in the Russian River watershed area. The HMT-West (hereafter HMT) enabled atmospheric scientists to investigate the role of ARs in creating flood-producing heavy precipitation (Ralph et al. 2004, 2006; Neiman et al. 2008; Ralph and Dettinger 2012).

The advantage of having consistent automated observations as a foundation, in addition to targeted weather-based field campaigns, remains clear to this day and has motivated CADWR to invest in the HMT-Legacy project, which addresses California's water and emergency management needs for weather and river forecasters and water managers (White et al. 2013). The locations of the existing HMT stations are shown in Fig. 1.

The third epoch: NOAA Habitat Blueprint. NOAA's Habitat Blueprint (NOAA 2019b) was designed to help restore and maintain healthy coastal and marine habitats through building on existing programs and adding new projects to address future priorities. In 2012, one of the first of ten regions to receive special emphasis as a NOAA Habitat Focus Area (NOAA 2019c) was California's Russian River. In 2008, NOAA's National Marine Fisheries Service had issued

a 15-yr Biological Opinion for endangered Coho and Chinook salmon and Steelhead in the Russian River and its tributaries. The Biological Opinion required the Sonoma Water and the U.S. Army Corps of Engineers (USACE) to work on a path toward building a healthy and sustainable habitat for these endangered species. This requirement includes changes in the minimum Russian River instream flows per California State Water Resources Control Board's Decision 1610 (State Water Resources Control Board 1986).

One of the projects awarded to the Russian River Focus Area was aimed at improving frost predictions and protection methods for vineyards (Chabot et al. 2016; Reynolds et al. 2016). During spring, vineyards withdrew water from streams to spray the budding vines to protect them from damaging frost. A large number of vineyards existed in the region, enough that widespread spraying could cause reduced stream flows, impacting fish habitats. Frost events in 2008 resulted in rapid depletion of the stage of the Russian River and some tributaries in Alexander Valley and Mendocino County. These rapid stage depletions resulted in juvenile salmonid deaths due to stranding.

In response, funding was provided to NOAA's Physical Sciences Division (PSD) to develop an advanced frost prediction tool. Advanced forecasting capabilities of frost events, including inversion conditions, could help coordinate reservoir releases and water diversions by vineyard managers to reduce the risk of harm to salmonids. The tool took advantage of local observations as well as a variety of forecast models to determine which models were providing the best skill at predicting frost (Reynolds et al. 2016). To increase the observational data that would be available for the tool and to provide real-time data for vineyard managers, the University of California (UC) Cooperative Extension program installed 20 inversion monitoring towers that measured the temperature gradient in the lowest 20 m. PSD installed data communications equipment and rain gauges at the tower sites to help make the inversion tower data readily available and to enhance the value of the tower sites during the wet season. Figure 1b shows the monitoring network that was available during the study.

Unfortunately, funding was no longer available to support the ongoing operation and maintenance of the forecasting tool, inversion towers, rain gauges, and data communications. Consequently, the program has ended and the observations are no longer available. Most of the wineries now rely on private sector weather providers who tailor their forecasts to the needs of the vintners. Nevertheless, alongside the FIRO program, the Russian River Habitat work has helped motivate the Sonoma Water to fund PSD and CW3E to install soil moisture monitoring stations around Lake Mendocino, one of the two reservoirs on the Russian River cooperated by USACE and Sonoma Water for flood control and water supply. Antecedent soil moisture can play an important role in determining runoff potential (e.g., Castillo et al. 2003; Cao et al. 2019).

The fourth epoch: FIRO. FIRO is a principal example of the integration of research and operations, in which meteorologists, hydrologists, civil engineers, biologists, economists, and decision-makers from various academic institutions and government agencies collaborate to achieve a water storage and distribution management goal (CW3E 2017). The FIRO program currently consists of two phases: FIRO-1 (Jasperse et al. 2017) and FIRO-2. FIRO-1 was launched in 2015 as a 5-yr program. It leverages modern weather and water forecasting skills and technologies to optimize Lake Mendocino reservoir operations, serving as both flood control (managed by the USACE) and water supply storage (managed by Sonoma Water). The operational viability of FIRO-1 was initially demonstrated in the Preliminary Viability Assessment (Jasperse et al. 2017) and will be concluded in the Final Viability Assessment by the end of WY 2020. FIRO-2 was launched in summer 2019 as a follow-on effort of FIRO-1 (more details in the "FIRO beyond the Russian River watershed" section).

Examples of FIRO-1 (hereby FIRO) operations include Russian River system management and planning for water releases from Lake Mendocino reservoir and for maintaining minimum downstream flows to support water supply, agriculture, recreation, and ecosystem needs. To meet these obligations, a wide variety of hydrometeorological observations, such as precipitation, soil moisture, streamflow, reservoir level and storage, and interagency collaborations from federal to local government entities as well as academia are necessary. The increasing utilization of these networks in near–real time by Sonoma Water, USACE, and other flood and fire emergency response organizations further demonstrate the significance of these hydrometeorological observation networks. The sensor network associated with FIRO is displayed in Fig. 1b.

The addition of Sonoma Water's OneRain network to RHONET after the devastating wildfires of 2017 (Mass and Ovens 2019) is another significant example. The network was established following the National Weather Service's (NWS's) and California Department of Forestry and Fire Protection's (CalFire's) recommendation to provide additional information regarding watershed conditions within and surrounding the burn areas, in order to better assess risks from flooding and debris flows (Sonoma Water 2019). Ultimately, the goal is to inform early flood warning systems, since there is a greater risk of flash floods and debris flows resulting from precipitation on burn scars similar to that documented in Southern California (Oakley et al. 2017).

The current state of Russian River hydrometeorological sensor network

This section will describe in some detail the many existing hydrometeorological monitoring networks in the Russian River basin. As described above, this watershed is densely instrumented and has benefitted from significant research investment over many years. This investment has supported various scientific and management objectives, e.g., enhancing preparedness through improved monitoring in response to extremes, such as floods, drought, and wildfire.

One unique characteristic of the hydrometeorological observation networks in the Russian River basin is the support for their deployment and maintenance from many different sectors of the economy and population. This includes leadership and cooperative involvement from research institutions such as the UC San Diego's CW3E, local, state, and federal agencies such as Sonoma Water, Potter Valley Fire Department, the City of Ukiah, CADWR, California Department of Transportation (CalTrans), Bureau of Land Management (BLM), and USACE, and private landowners, ranchers, farmers, and other groups. Instrument deployments by CW3E at an existing HMT site in Potter Valley and at a local ranch, as well as at the newly instrumented Deerwood and Boyes Creek Canyon exemplify such efforts (Figs. 4a–d).

Major hydrometeorological networks that have sites in this watershed include 1) USGS surface water and groundwater measurements; 2) CW3E instrumentation deployed in support of FIRO; 3) Sonoma Water's Automated Local Evaluation in Real Time (ALERT2)-based OneRain network; 4) NOAA HMT; 5) EFREP stations including AR observatories (AROs) Doppler wind profilers (Fig. 4e), vertically pointing S-band radars, and Advanced Quantitative Precipitation Information (AQPI) scanning X-band radars; and 6) miscellaneous intensive observing sites such as the Pepperwood Preserve, UC Davis Bodega Marine Laboratory (BML), and the Hopland Research and Extension Center (REC) (Fig. 1a). Other networks with observing sites in or around the watershed but not specific to hydrometeorological research and operations include the California Irrigation Management Information System (CIMIS) and the CalFire.

There are additional plans to continue instrumenting this watershed, for example, with a C-band scanning radar planned for installation in Sonoma and Marin Counties as part of AQPI. These networks are leveraged in order to support various science and management goals; such as flood forecasting and water supply management. There are also a number of seasonal observing systems put in place during the winter season when most precipitation

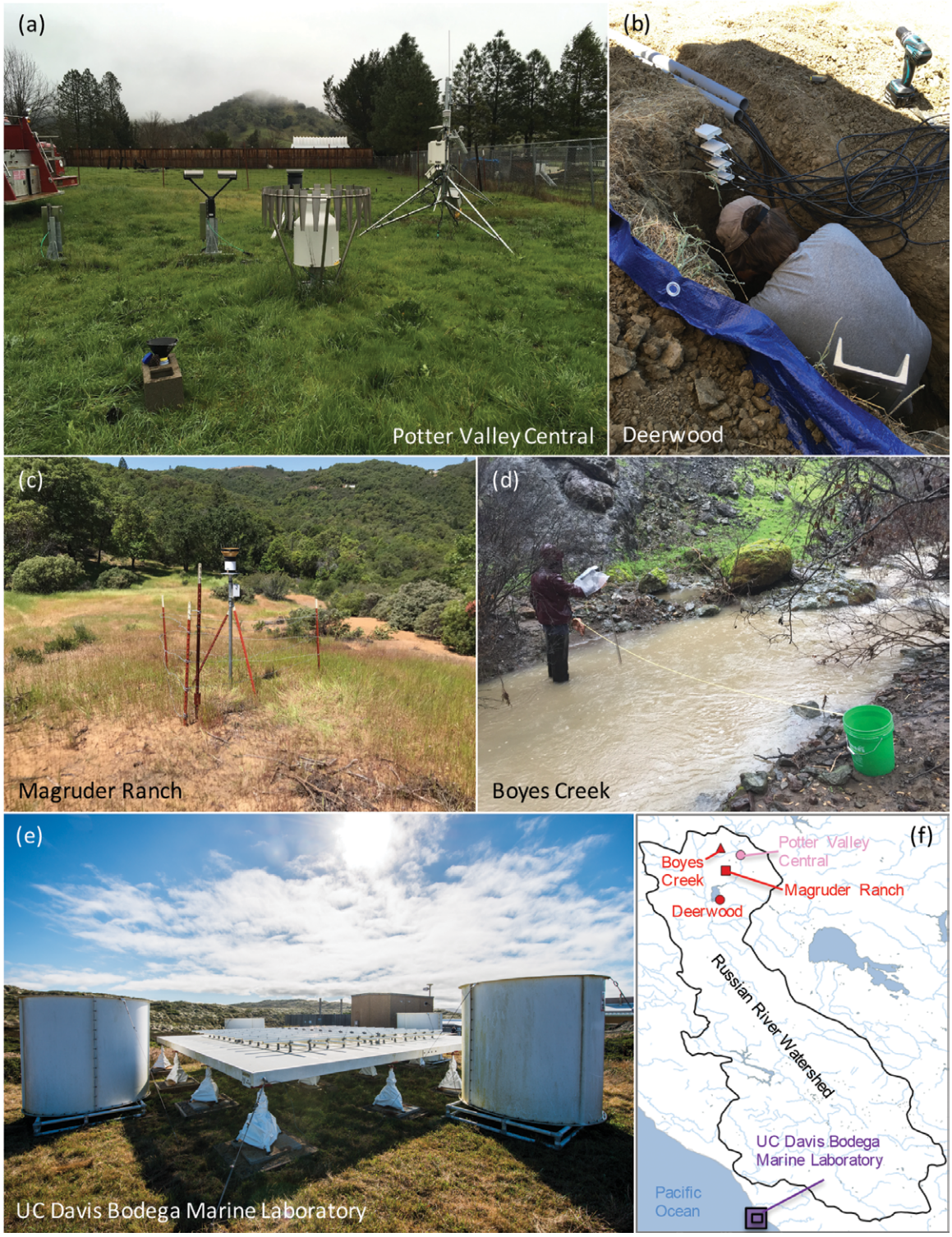

Fig. 4. (a) HMT Potter Valley Central site (39.3209°N, 123.102°W) with air temperature, relative humidity, precipitation, and soil temperature and moisture measurements. CW3E has also deployed a disdrometer, a weighing rain gauge, GPS-Met, a vertically pointing radar (not shown), and ISCO rainwater sampler during select storms (not shown) at the site. (b) CW3E telemetered soil moisture probe installation at Deerwood (39.1977°N, 123.1599°W) during the 2017 field campaign. (c) CW3E precipitation gauge at the Magruder Ranch in the Potter Valley area (39.2784°N, 123.1432°W). (d) CW3E stream gauging site at Boyes Creek (39.3405°N, 123.1635°W). A field technician is conducting manual stream gauging for rating curve development during the 2018 field campaign. (e) ARO 449-MHz wind profiler at UC Davis BML (38.3191°N, 123.0728°W). Image by CADWR. (f) Map showing the locations of the five sites in the Russian River watershed.

arrives, such as airborne reconnaissance of storms when they are offshore (White et al. 2013; Ralph et al. 2014), and radiosonde observations during storms when they make landfall in the watershed (Ralph et al. 2019a,b).

Since this paper focuses primarily on precipitation, soil moisture, and streamflow measurements being taken in the Russian River watershed, this section will now describe the measurement principles and siting considerations for networks that measure those important variables. In particular, the high density of precipitation and soil moisture observations in the Russian River is uniquely positioned to support ongoing hydrologic modeling efforts and to assess spatiotemporal variability of the landscape response to precipitation. A brief overview of other networks in the Russian will be provided first and then a focus will be placed on the more recent deployments in the upper Russian River watershed in support of FIRO objectives.

Russian River streamflow data are generally collected with the science goal of supporting water and hazard management and environmental research. For instance, USGS and Sonoma Water have cooperated to maintain stream gauges deployed in this watershed, which serve as the backbone for reservoir and river managements. Critically, these stream gauges' data support the Ensemble Forecast Operations (EFO)—a risk-based decision support system developed together with the California Nevada River Forecast Center (CNRFC) for flood control operations (Delaney et al. 2020). The EFO is leveraged in the Russian River Decision Support System (RR-DSS) as a tool to supplement USACE's spreadsheet and Corps Water Management System models (Fig. 5), in order to guide reservoir operations under FIRO. The RR-DSS includes a Hydrologic Engineering Center's Reservoir System Simulation (HEC-ResSim; USACE 2020) implementation and the Sonoma Water decision support model. The latter is modeled after the Yuba–Feather Forecast Coordinated Operations (Yuba Water Agency 2020) interface that resides on California Data Exchange Center (CDEC) and is operationally supported by the CADWR. This system has provided USACE operators with real-time modeling and analysis to assist managing water retained in the flood control pool, as requested by the major deviation (USACE 2018).

Soil moisture and precipitation data are collected to support similar goals, along with supporting weather and hydrologic modeling, and a particular focus for some sites on assisting irrigators in managing their water. The recent instrumentation of vulnerable areas (e.g., to fire and flood) of the watershed by the Sonoma Water also involved NOAA, as a part of the HMT program. The mission of HMT is to build resiliency to the impacts of extreme precipitation and to increase preparedness by improving integrated environmental forecast services, and in regard to soil moisture, understand the changes in soil moisture associated with the presence or absence of heavy precipitation events at multiple time scales (Zamora et al. 2011).

The CW3E instrumentation was added more recently in order to augment existing observations and monitoring of the hydrometeorology of the watershed. Specifically, the objectives were to better observe the upper watershed during cool-season AR events, which can result in heavy precipitation, saturated soils, and high streamflow rates. The goals considered when siting instrumentation were as follows:

1) Complement atmospheric observations made as part of other research projects, including dropsonde releases offshore as part of AR reconnaissance (Ralph et al. 2019b), radiosonde launches at Ukiah, California, and in Bodega Bay, California, radar observations of the vertical profile of hydrometeors, and disdrometer observations of precipitation phase and drop size distribution.
2) Improve understanding of the spatial variability of precipitation, soil moisture, and streamflow within the watershed to inform hydrologic model forecasts of streamflow during ARs, such as the USACE's Gridded Surface Subsurface Hydrologic Analysis (GSSHA) hydrologic model and NOAA's National Water Model (NWM).

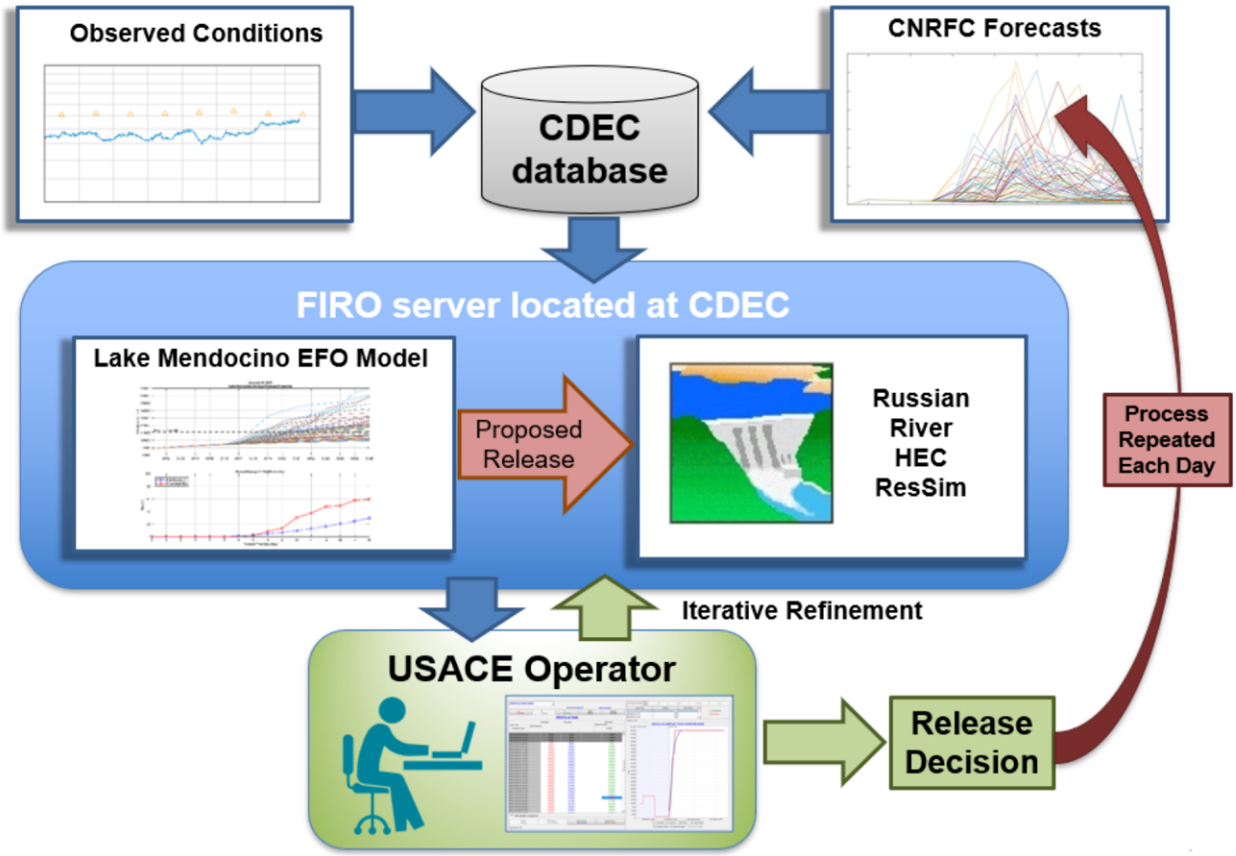

Fig. 5. The RR-DSS process flowchart.

3) Complement existing research observations of precipitation and soil moisture being made in the watershed as part of the NOAA HMT program, which has deployed instrumentation at four existing locations. The instrumentation hardware newly installed by CW3E was the same as the HMT sites for the purpose of augmenting the network.
4) Contribute to answering science questions about physical processes in AR-driven orographic precipitation in complex coastal terrain.
5) Provide near-real-time data on hydrometeorological conditions within the watershed to provide operational value to partners making decisions on reservoir operations.

Overall, the distribution of sensor networks in the Russian River reflects a dense area coverage, but many sensors do not have climatologically long periods of record. The upper Russian River watershed around the Lake Mendocino area has a high network density relative to the rest of the nation to inform reservoir management and operation related to FIRO.

The body of research on precipitation and hydrology in the Russian River provides an excellent foundation upon which to build, leveraging the expanded network of observations that provide exceptional, rich information on the watershed baseline conditions and response to extreme atmospheric moisture flux events. The next two sections of the paper will highlight how the available observations enhance our understanding of the incoming precipitation and hydrologic response of the watershed using in the next section an example of an AR that affected a large swath of the western United States, including the Russian River watershed, during April 2018 (Hatchett 2018), and in the "Examples of relevance to the broader hydrometeorological community" section an overview of the research advances that have been made possible with this network.

Case study: Lake Mendocino storage response during the April 2018 AR event

This case study demonstrates the capability of RHONET to capture soil moisture response to precipitation and its modulating effects on runoff/stream discharge and on Lake Mendocino reservoir storage. We specifically utilize the precipitation and soil moisture content at 10-cm-depth records from Boyes Creek Canyon, as well as the stream discharge records from Boyes Creek, five other CW3E tributary stream gauges and a downstream USGS stream gauge located in Calpella. Additionally, we employ storage level and rule curve thresholds separating the water supply and flood control operations from the Lake Mendocino reservoir. Other datasets from RHONET can also provide useful information. However, this case study serves as a brief example of the use of RHONET in hydrometeorological analysis during an extreme weather event; any more detailed analyses are beyond the scope of the study.

The period of analysis is the early April 2018 AR event, which was associated with two phases of precipitation occurring in late 5 April and early 7 April 2018 (Fig. 6). This event was characterized by a strong, warm AR making landfall in the Russian River basin area, following a relatively dry winter. The event resulted in the replenishment of Lake Mendocino from a sizeable deficit in water storage (~13% from the storage target) and was associated with the rapid snow ablation and flooding farther inland in the Yosemite Valley (National Park Service 2018; Hatchett 2018).

During the first phase of the event, the volumetric soil moisture records at 10-cm depth from nine CW3E and HMT sites in the Lake Mendocino subbasin (~270-km^2 catchment area; CDEC 2017) saw 7%–54% increases within 6 h, between 0400 and 1000 UTC 6 April 2018. These increases lagged 3–10 h behind the start of the precipitation at 2100 UTC 5 April 2018. This behavior illustrates the strong precipitation influence on soil moisture fluctuations, despite the variations in the magnitude and the timing of the soil moisture responses across the area.

After 1200 UTC 6 April 2018, soil moisture increased more slowly and stream discharge started to increase, as the soil had reached saturation and surface runoff generation had started. The hydrographs from six tributary gauges spread across the upper Russian River basin exhibited uniform responses to precipitation, with virtually no time lag between each other. The hydrograph from a downstream USGS gauge at Calpella exhibited a ~1-h delay with respect to the 6 tributaries, reflecting its role as a convolution of upstream tributaries. A few hours following the stream response, the storage level in Lake Mendocino increased rapidly, but was still well below the target water supply storage (by ~10% at the end of 6 April 2018).

As the precipitation rate decreased toward the end of 6 April 2018, the stream hydrographs receded and the Lake Mendocino storage level increased modestly. The second phase of the event started at 0300 UTC 7 April 2018. The streams and reservoir responded almost immediately, since the soil was saturated relative to the beginning of the first phase. The event concluded by 1200 UTC 7 April 2018, marked by the precipitation cessation and rapid declines in the stream hydrographs. Nevertheless, Lake Mendocino's storage level continued to increase, though more slowly, until 10 April 2018 when the storage level started to plateau. Overall, the full reservoir storage response to the precipitation event took place roughly over a period of 5 days. The storage gained ~1.4×10^7 m^3 (16%) of storage throughout the event and attained the target water supply storage by 1500 UTC 11 April 2018.

This result exemplifies the role of antecedent soil conditions in modulating precipitation–runoff process, which can delay the runoff and provides a buffer against flood. Nonetheless, soil moisture and streamflow responses to precipitation can vary significantly over a relatively small area and within a few hours, corroborating the importance of spatially and temporally dense observations.

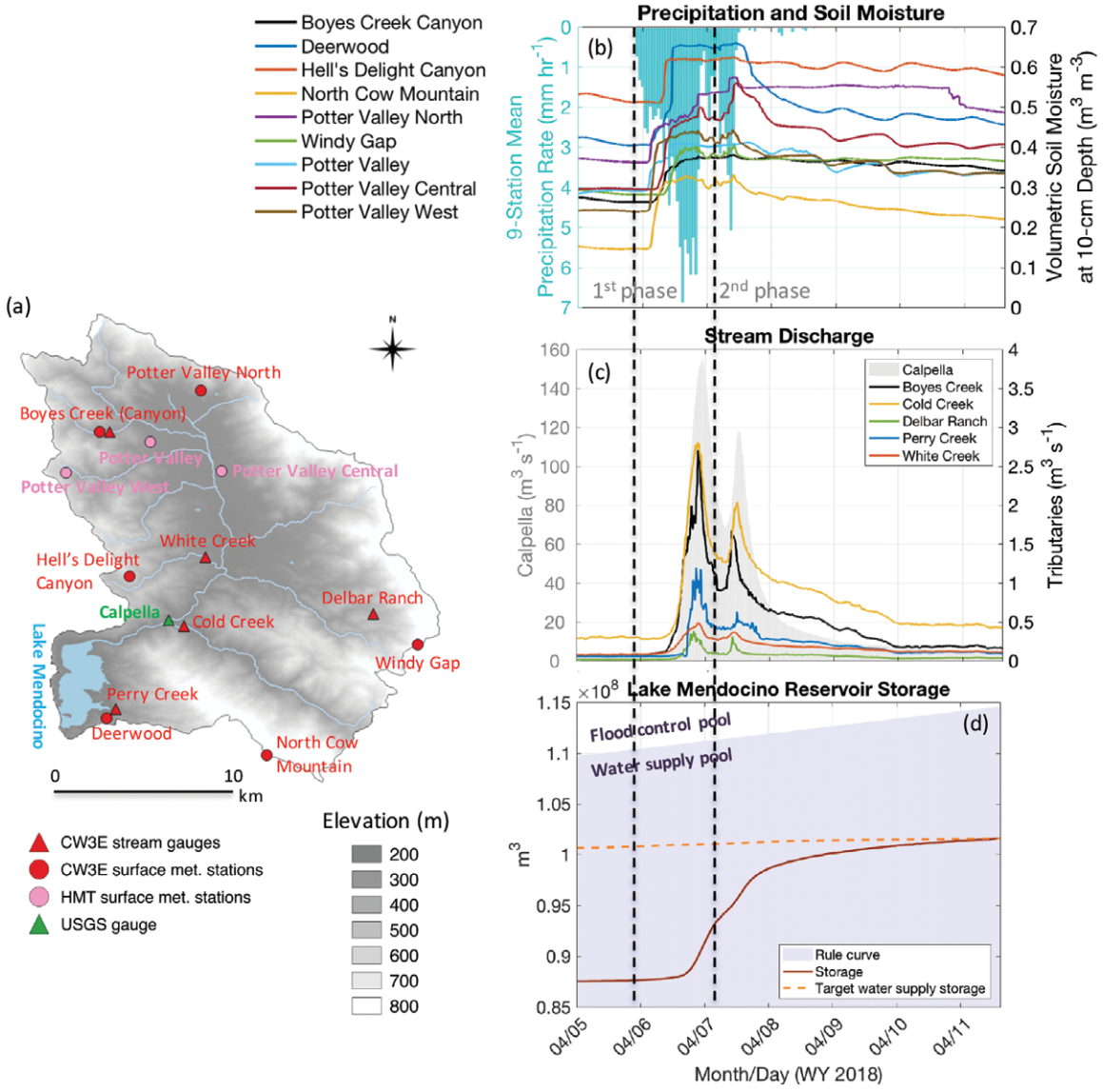

Fig. 6. (a) Terrain base map showing the locations of stream gauge and surface meteorological stations in the Lake Mendocino area. (b) Time series (UTC) of mean hourly precipitation rate and 2-min soil moisture volumetric water content at 10-cm depth at nine CW3E and HMT stations during the early April 2018 AR event. (c) The 15-min stream discharge time series from the USGS Russian River gauge at Calpella and six CW3E tributary stream gauges. (d) Daily curve storage, hourly storage, and target water supply storage at Lake Mendocino. The storage and rule curves are provided by the Sonoma Water and tabulated on CDEC. The target storage curve is the optimal storage level as a function of the time of year (Sonoma Water 2018b).

Examples of relevance to the broader hydrometeorological community

Development of nonbrightband rain detection. In analyzing the vertically pointing S-band precipitation profiling radar (S-PROF) data from the coastal mountains above the town of Cazadero in Northern California, White et al. (2003) developed an algorithm to distinguish between nonbrightband (NBB) rain and its much deeper counterpart brightband rain using the automated brightband detection algorithm developed by White et al. (2002). This precipitation process partitioning algorithm and its results have been used in subsequent studies (Neiman et al. 2005; Kingsmill et al. 2006, 2016; Martner et al. 2008; Coplen et al. 2008, 2015; Matrosov et al. 2014, 2016; White et al. 2015; Bytheway et al. 2019) relating to NBB rain, as well as the role of aerosols in creating and/or enhancing precipitation (Ault et al. 2011; Creamean et al. 2013, 2016; Martin et al. 2019a), within and beyond the Russian River region.

In addition, as demonstrated by White et al. (2003) and Martner et al. (2008), the microphysical properties of NBB rain are significantly different from brightband rain, such that traditional rainfall estimates using a reflectivity–rain rate (Z–R) relationship calibrated to stratiform rain dramatically underestimate NBB rain rates. In some cases, this setback renders quantitative precipitation estimates (QPE) using the U.S. operational precipitation scanning radar (WSR-88D) network inadequate for this part of the California's coastal topography.

This issue is a primary motivation for the AQPI project funded by the CADWR. The AQPI project will install several gap-filling radars in the San Francisco Bay Area (SFBA), including in Sonoma County where the S-PROF radar above Cazadero has been operating nearly continuously since CALJET. Importantly, this addition will enhance the near-term precipitation forecasting capability and assist public agencies in preparing for flood events. Other S-PROF radars from NOAA's Earth System Research Laboratory (ESRL) are currently operating in the SFBA at Middletown, Santa Rosa, and Twitchell Island, as well as farther south at Point Sur. A newer type of S-band precipitation profiler known as a snow-level radar (SLR) has been developed by NOAA/ESRL (Johnston et al. 2017). Eleven of these SLRs are located in major watersheds across California and supported by CADWR. Like the S-PROF, the SLR provides vertical profiles of radar reflectivity that can aid scanning radars with QPE using a vertical profile of reflectivity correction (Chen et al. 2019). The AQPI project can serve as a template for other populated regions that need finer-scale and more accurate QPE and quantitative precipitation forecasts, especially during extreme events.

Global growth in AR-related studies. ARs are major drivers to precipitation in the Russian River watershed, bringing both beneficial and hazardous precipitation. However, the hydrologic impacts of ARs have been identified all over the globe, from the United States (Table 2) to the United Kingdom (Lavers et al. 2011) and continental Europe (Stohl et al. 2008; Lavers and Villarini 2013), to Chile (Garreaud 2013), to Japan (Hirota et al. 2016), and to New Zealand (Little et al. 2019). The explosive increase in the number of publications covering or mentioning ARs over the past several years reflects this phenomenon (Ralph et al. 2017; Wilson et al. 2019). The process-based understanding enabled by densely instrumented watersheds, such as the Russian River, is invaluable in understanding the detailed life cycle of ARs after they make landfall. They may also help to understand the key modulators of AR impacts based on watershed characteristics and other factors, and provide guidance that can inform the design of other watershed-based hydrometeorological monitoring networks.

FIRO beyond the Russian River watershed. There has also been an expanded interest in the potential application of FIRO in other watersheds, especially those with precipitation regimes strongly affected by ARs. Currently, FIRO viability is under exploration at Prado Dam in the Santa Ana watershed in Southern California, and at the Oroville Dam and New Bullards Bar Reservoir in the Yuba and Feather River watersheds. These watersheds were chosen in particular for their differences from Lake Mendocino, in the context of gaps in meteorological and hydrological forecast skill, which could yield new insights into FIRO benefits and applications.

Santa Ana was chosen because ARs behave differently in Southern California than in Northern California (Cannon et al. 2018). The Yuba–Feather watersheds were chosen as they bring in consideration such as higher terrain and the need to understand and forecast snow processes. Both watersheds have different characteristics such as size, terrain, land use, and other factors that may be important for FIRO viability. All FIRO efforts in new watersheds are structured following the model of Lake Mendocino FIRO, with steering committees including representatives from a range of stakeholders, researchers, and operations (Talbot et al. 2019).

Table 2. Examples of research topics and the associated publications emerging from the use of RHONET since its conception.

Topic	Key publication(s)
Role of landfalling ARs in flood generation	Ralph et al. (2004, 2005a, 2006), Neiman et al. (2008), Dettinger et al. (2011), Ralph and Dettinger (2012), Cao et al. (2019), Han et al. (2019)
Shallow nonbrightband rainfall	White et al. (2003), Kingsmill et al. (2006, 2016), Martner et al. (2008), Matrosov et al. (2014), Coplen et al. (2015), Bytheway et al. (2019)
Buffering role of dry antecedent soil condition	Ralph et al. (2006, 2013a), Cao et al. (2019)
Forecast-informed reservoir operations	Jasperse et al. (2017)

Over the next phase of FIRO, investigations will continue into the already identified watersheds. In addition, additional reservoirs will be chosen both for full viability assessments and for screening level assessments. The procedure for conducting screening-level assessments will be an important development, as interest in FIRO continues to rise. These screening assessments will provide guidelines for how to determine whether it is worth the time and effort to implement a full FIRO viability assessment across a much broader range of meteorological and hydrological regimes than that explored in the first several reservoirs. The lessons from Lake Mendocino, and, as particularly relevant here, the requirements for an appropriately dense monitoring network, will be applied to the new watersheds.

Research and operational benefits

Creation of rich hydrometeorology datasets, such as the one described herein, provides valuable information for stakeholders, water and emergency management operations, and research and development. Throughout the western United States, water resources remain a critical component of the livelihood, economy, ecology, and agricultural productivity of the region, all while being subjected to overall larger demand. Fundamentally, any guidance to operations and management of these limited water resources in the western United States should be informed by a thorough understanding of atmospheric processes related to the precipitation generation in reservoir/river catchments, as well as the land surface uptake behavior of that precipitation over time.

From the research perspective, data from networks with long-term, densely sampled, high-temporal-resolution instrumentation—that ultimately capture the diversity of the watershed or region—are a key component to addressing gaps in technology and/or hydrometeorological understanding (Table 2). For example, ground-based precipitation datasets are essential components of QPE, especially in this region where NWS's radars are frequently blocked at low levels, where significant precipitation may be occurring (Matrosov et al. 2014; Bytheway et al. 2019). Distributed ground observations of precipitation have been widely used to evaluate precipitation forecasts (e.g., Ralph et al. 2010; Sukovich et al. 2014; Martin et al. 2018) as well as field-campaign-deployed radar-based QPE (e.g., Gourley et al. 2009; Zhang et al. 2012; Lim et al. 2013; Willie et al. 2017). Importantly, these observations have helped improve the precipitation forecast in the Russian River watershed (Martin et al. 2018). Such datasets have also advanced broadscale characterization of orographic-precipitation processes associated with ARs (e.g., Ralph and Dettinger 2011; Ralph et al. 2013a,b, 2016b; Chen et al. 2019) and their associated impact on flood and drought (e.g., Ralph et al. 2006). Significant advances in understanding the relationship of antecedent soil moisture to runoff generation in flood prone areas have also been made possible using these monitoring legacy networks (e.g., Zamora et al. 2011; Ralph et al. 2013a; Cao et al. 2019).

The diversity of the observations within these rich networks also supports cross-disciplinary approaches to hydrometeorological modeling challenges in calibration, verification, and physical process parameterization development. Adequate calibration of hydrologic parameters in models relies, in part, on the quality of the sources of observations or meteorological forcing datasets that replicate temporal and spatial variability during important hydrologic events (Beven and Binley 1992; Michaud and Sorooshian 1994; Yu et al. 1999; Yu 2000; Ajami et al. 2004). This factor is also accounted for in the ongoing GSSHA (Jasperse et al. 2017) and NWM (Han et al. 2019) model calibration efforts for the Russian River watershed. Hydrometeorology networks, including the HMT and CW3E described herein, are ultimately designed with the goal to capture the impacts of these hydrologic events and the varying degrees of heterogeneity in elevation, vegetation, and soil characteristics (Zamora et al. 2011). These observations have been and will continue to be leveraged in the validation process to identify potential biases in configuration or estimation of important hydrological processes (e.g., Zamora et al. 2013). Such information will help further isolate physical processes that modulate important precipitation characteristics, such as rainfall intensity, timing, and duration, and the land surface process response functions.

The operational sectors are supported by information provided via these hydrometeorological networks in order to create interagency strategic plans related to water resource management, sanitation, and emergency response coordination for drought, flood, and fire. For example, CW3E, Sonoma Water, and USACE collaboratively develop a major deviation request for Lake Mendocino reservoir operation (USACE 2018), which seeks to conditionally store additional water above the existing guide curve to improve the water supply reliability. This effort utilizes numerical models and RR-DSS that rely on inputs from RHONET (Fig. 5) to assess the adequacy of existing flood management infrastructure and to evaluate existing and future flood risk in the Russian River watershed.

Real-time stream gauge data, such as those from USGS and Sonoma Water's OneRain, are used to coordinate and manage reservoir releases to meet minimum instream flows in the Russian River as required by the State Water Resource Control Board. These instream flows support water supply, recreation, and ecosystems, particularly endangered salmonids. In addition, data from radiosondes, AROs (including vertical scanning wind profilers), frequency-modulated continuous-wave (FMCW), S-, X- and C-Band radars, rain gauges, soil moisture, and stream stage/flow help assess postfire hazards due to ARs such as debris flows, flash floods, and increased risk of flooding. Similarly, advances in forecasting of AR events benefit wastewater system operators to better prepare for addressing sanitary sewer overflows and minimizing their impacts (e.g., deployment of crews and equipment).

Conclusions and recommendations

The research and operational benefits of RHONET are realized through improved data collection and integrating observations from all different sources of information from the atmosphere to the surface and subsurface. In FIRO, for example, RHONET is a critical piece of "enhanced monitoring" and a support for modeling efforts to better understand the physical processes. The exercise of transferability (from one watershed to another) includes the assessment of watershed monitoring gaps. While these considerations are different for different watersheds (e.g., the relative importance of snow at Yuba–Feather watersheds), important lessons can emerge from the Russian River watershed. For instance, small-scale landscape heterogeneity can be significant and we need to strive for representative measurements in different soil types, slope, and elevation.

Over the long term, such a network can help identify the dominant physical processes and their variabilities at different spatial and temporal scales (Lundquist et al. 2016) and the optimal monitoring strategy (Curtis et al. 2019). It can also capture systemic changes

due to external perturbations, such as fires (Ren et al. 2011; Hubbert et al. 2012) and floods (Ortega et al. 2014). Ultimately, such a monitoring system can enhance operational capabilities, e.g., by enabling data sharing and management among stakeholders and by enhancing data visualization and watershed runoff modeling capabilities (Jasperse et al. 2017).

Finally, it is important that utilities, research agencies, and others involved in developing and maintaining observational networks coordinate and form relationships with entities typically involved with emergency response and public safety and managing and operating telecommunication systems for reliable and secure transfer of data, especially during critical times of need. Maintaining adequate funding for such observation networks and operations, which continues to be a challenge, is crucial to ensure reliable communication and emergency responses during extreme events.

Acknowledgments. This work is supported by the USACE Army Engineer Research and Development Center (Award W912HZ-15-2-0019) and the NOAA Hydrometeorology Testbed (Award NA17OAR4590185) programs. We thank Caroline Ellis, Douglas Alden, Robert Hartman, and many others involved in the Russian River basin fieldwork for measurement data retrieval and processing. We also thank Chris Delaney, Carlos Diaz, and John Mendoza at Sonoma Water for providing the Lake Mendocino reservoir data. Finally, we are thankful to the BLM, CalTrans, City of Ukiah, Potter Valley Fire Department, UC Davis BML, USACE, and many Mendocino County community members that have provided permission to locate, store, and maintain sensors on their land, including the Paulises, the Magruders, the Farmers, the Strohs, the Delbars, and the Pipers.

Data availability statement. ARO, EFREP/AQPI, and HMT data are available on the NOAA/PSD website (NOAA 2019a). CDEC dataset is available on the CDEC website (CDEC 2017). CW3E surface meteorological data are available on the CW3E website (CW3E 2019) and on the NOAA/PSD website (NOAA 2019a), under the "Scripps (CW3E)" option on Data Source dropdown menu. Additional dataset pertaining to CW3E stream gauges discharge and the case study can be accessed on Sumargo et al. (2020) repository at https://doi.org/10.4211/hs.3c3a2f3d491c4e4aa4ccb6764806eb8a. Any inquiries on CW3E observation data can be directed to cw3e-fieldwork-g@ucsd.edu. PRISM dataset is available from the PRISM Climate Group website (PRISM Climate Group 2019). Sonoma Water data are available on the their OneRain website (Sonoma Water 2019). The USGS dataset is available on the USGS website (USGS 2019).

References

Ajami, N. K., H. Gupta, T. Wagener, and S. Sorooshian, 2004: Calibration of a semi-distributed hydrologic model for streamflow estimation along a river system. *J. Hydrol.*, **298**, 112–135, https://doi.org/10.1016/j.jhydrol.2004.03.033.

Ault, A. P., C. R. Williams, A. B. White, P. J. Neiman, J. M. Creamean, C. J. Gaston, F. M. Ralph, and K. A. Prather, 2011: Detection of Asian dust in California orographic precipitation. *J. Geophys. Res.*, **116**, D16205, https://doi.org/10.1029/2010JD015351.

Beven, K., and A. Binley, 1992: The future of distributed models: Model calibration and uncertainty prediction. *Hydrol. Processes*, **6**, 279–298, https://doi.org/10.1002/hyp.3360060305.

Bytheway, J. L., M. Hughes, K. Mahoney, and R. Cifelli, 2019: A multiscale evaluation of multisensor quantitative precipitation estimates in the Russian River basin. *J. Hydrometeor.*, **20**, 447–466, https://doi.org/10.1175/JHM-D-18-0142.1.

Cannon, F., F. M. Ralph, A. M. Wilson, and D. P. Lettenmaier, 2017: GPM satellite radar measurements of precipitation and freezing level in atmospheric rivers: Comparison with ground-based radars and reanalyses. *J. Geophys. Res. Atmos.*, **122**, 12 747–12 764, https://doi.org/10.1002/2017JD027355.

——, C. Hecht, J. Cordeira, and F. M. Ralph, 2018: Synoptic to mesoscale forcing of extreme precipitation in Southern California. *J. Geophys. Res. Atmos.*, **123**, 13 714–13 730, https://doi.org/10.1029/2018JD029045.

Cao, Q., A. Mehran, F. M. Ralph, and D. P. Lettenmaier, 2019: The role of hydrologic initial conditions on atmospheric river floods in the Russian River basin. *J. Hydrometeor.*, **20**, 1667–1686, https://doi.org/10.1175/JHM-D-19-0030.1.

Castillo, V. M., A. Gómez-Plaza, and M. Martínez-Mena, 2003: The role of antecedent soil water content in the runoff response of semiarid catchments: A simulation approach. *J. Hydrol.*, **284**, 114–130, https://doi.org/10.1016/S0022-1694(03)00264-6.

CDEC, 2017: Dam profile for Coyote (Lake Mendocino). Accessed 1 June 2019, http://cdec.water.ca.gov/dynamicapp/profile?s=COY&type=dam.

Chabot, H., D. Farrow, D. York, J. Harris, N. Cosentino-Manning, L. Watson, K. Hum, and C. Wiggins, 2016: Thinking big: Lessons learned from a landscape-scale approach to coastal habitat conservation. *Coastal Manage.*, **44**, 175–192, https://doi.org/10.1080/08920753.2016.1160202.

Chen, H., R. Cifelli, and A. White, 2019: Improving operational radar rainfall estimates using profiler observations over complex terrain in Northern California. *IEEE Trans. Geosci. Remote Sens.*, **58**, 1821–1832, https://doi.org/10.1109/TGRS.2019.2949214.

Coplen, T. B., P. J. Neiman, A. B. White, J. M. Landwehr, F. M. Ralph, and M. D. Dettinger, 2008: Extreme changes in stable hydrogen isotopes and precipitation characteristics in a landfalling Pacific storm. *Geophys. Res. Lett.*, **35**, L21808, https://doi.org/10.1029/2008GL035481.

——, ——, ——, and F. M. Ralph, 2015: Categorisation of Northern California rainfall for periods with and without a radar brightband using stable isotopes and a novel automated precipitation collector. *Tellus*, **67B**, 28574, https://doi.org/10.3402/tellusb.v67.28574.

Corringham, T. W., F. M. Ralph, A. Gershunov, D. R. Cayan, and C. A. Talbot, 2019: Atmospheric rivers drive flood damages in the western United States. *Sci. Adv.*, **5**, eaax4631, https://doi.org/10.1126/SCIADV.AAX4631.

Creamean, J. M., and Coauthors, 2013: Dust and biological aerosols from the Sahara and Asia influence precipitation in the western U.S. *Science*, **339**, 1572–1578, https://doi.org/10.1126/science.1227279.

——, A. B. White, P. Minnis, R. Palikonda, D. A. Spangenberg, and K. A. Prather, 2016: The relationships between insoluble precipitation residues, clouds, and precipitation over California's southern Sierra Nevada during winter storms. *Atmos. Environ.*, **140**, 298–310, https://doi.org/10.1016/j.atmosenv.2016.06.016.

Curtis, J. A., L. E. Flint, and M. A. Stern, 2019: A multi-scale soil moisture monitoring strategy for California: Design and validation. *J. Amer. Water Resour. Assoc.*, **55**, 740–758, https://doi.org/10.1111/1752-1688.12744.

CW3E, 2017: Overview: Forecast informed reservoir operations. Accessed 22 April 2019, https://cw3e.ucsd.edu/firo/.

——, 2019: CW3E observation data. Accessed 23 December 2019, http://cw3e.ucsd.edu/images/CW3E_Obs/Data/.

Daly, C., R. P. Neilson, and D. L. Phillips, 1994: A statistical–topographic model for mapping climatological precipitation over mountainous terrain. *J. Appl. Meteor.*, **33**, 140–158, https://doi.org/10.1175/1520-0450(1994)033<0140:ASTMFM>2.0.CO;2.

——, M. Halblieb, J. I. Smith, W. P. Gibson, M. K. Doggett, G. H. Taylor, J. Curtis, and P. P. Pasteris, 2008: Physiographically sensitive mapping of climatological temperature and precipitation across the conterminous United States. *Int. J. Climatol.*, **28**, 2031–2064, https://doi.org/10.1002/joc.1688.

Delaney, C. J., and Coauthors, 2020: Forecast informed reservoir operations using ensemble streamflow predictions for a multipurpose reservoir in Northern California. *Water Resour. Res.*, **56**, e2019WR026604, https://doi.org/10.1029/2019WR026604.

Dettinger, M. D., F. M. Ralph, T. Das, P. J. Neiman, and D. R. Cayan, 2011: Atmospheric rivers, floods and the water resources of California. *Water*, **3**, 445–478, https://doi.org/10.3390/w3020445.

Flint, L. E., A. L. Flint, J. Mendoza, J. Kalansky, and F. M. Ralph, 2018: Characterizing drought in California: New drought indices and scenario-testing in support of resource management. *Ecol. Process.*, **7**, 1, https://doi.org/10.1186/s13717-017-0112-6.

Fritsch, J. M., and R. E. Carbone, 2004: Improving quantitative precipitation forecasts in the warm season: A USWRP research and development strategy. *Bull. Amer. Meteor. Soc.*, **85**, 955–966, https://doi.org/10.1175/BAMS-85-7-955.

Garreaud, R., 2013: Warm winter storms in central Chile. *J. Hydrometeor.*, **14**, 1515–1534, https://doi.org/10.1175/JHM-D-12-0135.1.

Gershunov, A., and Coauthors, 2019: Precipitation regime change in western North America: The role of atmospheric rivers. *Sci. Rep.*, **9**, 9944, https://doi.org/10.1038/S41598-019-46169-W.

Gourley, J. J., D. P. Jorgensen, S. Y. Matrosov, and Z. L. Flamig, 2009: Evaluation of incremental improvements to quantitative precipitation estimates in complex terrain. *J. Hydrometeor.*, **10**, 1507–1520, https://doi.org/10.1175/2009JHM1125.1.

Han, H., J. Kim, V. Chandrasekar, J. Choi, and S. Lim, 2019: Modeling streamflow enhanced by precipitation from atmospheric river using the NOAA National Water Model: A case study of the Russian River basin for February 2004. *Atmosphere*, **10**, 466, https://doi.org/10.3390/atmos10080466.

Hatchett, B. J., 2018: Snow level characteristics and impacts of a spring typhoon-originating atmospheric river in the Sierra Nevada, USA. *Atmosphere*, **9**, 233, https://doi.org/10.3390/atmos9060233.

Hirota, N., Y. N. Takayabu, M. Kato, and S. Arakane, 2016: Roles of an atmospheric river and a cutoff low in the extreme precipitation event in Hiroshima on 19 August 2014. *Mon. Wea. Rev.*, **144**, 1145–1160, https://doi.org/10.1175/MWR-D-15-0299.1.

Hubbert, K. R., P. M. Wohlgemuth, J. L. Beyers, M. G. Narog, and R. Gerrard, 2012: Post-fire soil water repellency, hydrologic response, and sediment yield compared between grass-converted and chaparral watersheds. *Fire Ecol.*, **8**, 143–162, https://doi.org/10.4996/fireecology.0802143.

Jasperse, J., and Coauthors, 2017: Preliminary viability assessment of Lake Mendocino forecast informed reservoir operations. Center for Western Weather and Water Extremes Rep., 76 pp.

Johnston, P. E., J. R. Jordan, A. B. White, D. A. Carter, D. M. Costa, and T. E. Ayers, 2017: The NOAA FM-CW snow-level radar. *J. Atmos. Oceanic Technol.*, **34**, 249–267, https://doi.org/10.1175/JTECH-D-16-0063.1.

Kingsmill, D. E., P. J. Neiman, F. M. Ralph, and A. B. White, 2006: Synoptic and topographic variability of Northern California precipitation characteristics in landfalling winter storms observed during CALJET. *Mon. Wea. Rev.*, **134**, 2072–2094, https://doi.org/10.1175/MWR3166.1.

——, ——, B. J. Moore, M. Hughes, S. E. Yuter, and F. M. Ralph, 2013: Kinematic and thermodynamic structures of Sierra barrier jets and overrunning atmospheric rivers during a landfalling winter storm in Northern California. *Mon. Wea. Rev.*, **141**, 2015–2036, https://doi.org/10.1175/MWR-D-12-00277.1.

——, ——, and A. B. White, 2016: Microphysics regime impacts on the relationship between orographic rain and orographic forcing in the coastal mountains of Northern California. *J. Hydrometeor.*, **17**, 2905–2922, https://doi.org/10.1175/JHM-D-16-0103.1.

Lamjiri, M. A., M. D. Dettinger, F. M. Ralph, and B. Guan, 2017: Hourly storm characteristics along the U.S. West Coast: Role of atmospheric rivers in extreme precipitation. *Geophys. Res. Lett.*, **44**, 7020–7028, https://doi.org/10.1002/2017GL074193.

Lavers, D. A., and G. Villarini, 2013: The nexus between atmospheric rivers and extreme precipitation across Europe. *Geophys. Res. Lett.*, **40**, 3259–3264, https://doi.org/10.1002/grl.50636.

——, R. P. Allan, E. F. Wood, G. Villarini, D. J. Brayshaw, and A. J. Wade, 2011: Winter floods in Britain are connected to atmospheric rivers. *Geophys. Res. Lett.*, **38**, L23803, https://doi.org/10.1029/2011GL049783.

Lim, S., R. Cifelli, V. Chandrasekar, and S. Y. Matrosov, 2013: Precipitation classification and quantification using X-band dual-polarization weather radar: Application in the Hydrometeorology Testbed. *J. Atmos. Oceanic Technol.*, **30**, 2108–2120, https://doi.org/10.1175/JTECH-D-12-00123.1.

Little, K., D. G. Kingston, N. J. Cullen, and P. B. Gibson, 2019: The role of atmospheric rivers for extreme ablation and snowfall events in the Southern Alps of New Zealand. *Geophys. Res. Lett.*, **46**, 2761–2771, https://doi.org/10.1029/2018GL081669.

Lundquist, J. D., and Coauthors, 2016: Yosemite Hydroclimate Network: Distributed stream and atmospheric data for the Tuolumne River watershed and surroundings. *Water Resour. Res.*, **52**, 7478–7489, https://doi.org/10.1002/2016WR019261.

Martin, A. C., F. M. Ralph, R. Demirdjian, L. DeHaan, R. Weihs, J. Helly, D. Reynolds, and S. Iacobellis, 2018: Evaluation of atmospheric river predictions by the WRF Model using aircraft and regional mesonet observations of orographic precipitation and its forcing. *J. Hydrometeor.*, **19**, 1097–1113, https://doi.org/10.1175/JHM-D-17-0098.1.

——, and Coauthors, 2019a: Contrasting local and long-range-transported warm ice-nucleating particles during an atmospheric river in coastal California, USA. *Atmos. Chem. Phys.*, **19**, 4193–4210, https://doi.org/10.5194/acp-19-4193-2019.

——, F. M. Ralph, A. Wilson, L. DeHaan, and B. Kawzenuk, 2019b: Rapid cyclogenesis from a mesoscale frontal wave on an atmospheric river: Impacts on forecast skill and predictability during atmospheric river landfall. *J. Hydrometeor.*, **20**, 1779–1794, https://doi.org/10.1175/JHM-D-18-0239.1.

Martner, B. E., S. E. Yuter, A. B. White, S. Y. Matrosov, D. E. Kingsmill, and F. M. Ralph, 2008: Raindrop size distributions and rain characteristics in California coastal rainfall for periods with and without a radar bright band. *J. Hydrometeor.*, **9**, 408–425, https://doi.org/10.1175/2007JHM924.1.

Mass, C. F., and D. Ovens, 2019: The Northern California wildfires of 8–9 October 2017: The role of a major downslope wind event. *Bull. Amer. Meteor. Soc.*, **100**, 235–256, https://doi.org/10.1175/BAMS-D-18-0037.1.

Matrosov, S. Y., F. M. Ralph, P. J. Neiman, and A. B. White, 2014: Quantitative assessment of operational weather radar rainfall estimates over California's northern Sonoma County using HMT-West data. *J. Hydrometeor.*, **15**, 393–410, https://doi.org/10.1175/JHM-D-13-045.1.

——, R. Cifelli, P. J. Neiman, and A. B. White, 2016: Radar rain-rate estimators and their variability due to rainfall type: An assessment based on hydrometeorology testbed data from the Southeastern United States. *J. Appl. Meteor. Climatol.*, **55**, 1345–1358, https://doi.org/10.1175/JAMC-D-15-0284.1.

Michaud, J., and S. Sorooshian, 1994: Comparison of simple versus complex distributed runoff models on a midsized semiarid watershed. *Water Resour. Res.*, **30**, 593–605, https://doi.org/10.1029/93WR03218.

Morss, R. E., and F. M. Ralph, 2007: Use of information by National Weather Service forecasters and emergency managers during CALJET and PACJET-2001. *Wea. Forecasting*, **22**, 539–555, https://doi.org/10.1175/WAF1001.1.

National Park Service, 2018: Update for April 11, 2018. Accessed 30 August 2019, www.nps.gov/yose/blogs/update-for-april-11-2018.htm.

Neiman, P. J., F. M. Ralph, P. O. Persson, A. B. White, D. P. Jorgensen, and D. E. Kingsmill, 2004: Modification of fronts and precipitation by coastal blocking during an intense landfalling winter storm in Southern California: Observations during CALJET. *Mon. Wea. Rev.*, **132**, 242–273, https://doi.org/10.1175/1520-0493(2004)132<0242:MOFAPB>2.0.CO;2.

——, B. E. Martner, A. B. White, G. A. Wick, F. M. Ralph, and D. E. Kingsmill, 2005: Wintertime nonbrightband rain in California and Oregon during CALJET and PACJET: Geographic, interannual, and synoptic variability. *Mon. Wea. Rev.*, **133**, 1199–1223, https://doi.org/10.1175/MWR2919.1.

——, F. M. Ralph, A. B. White, D. D. Parrish, J. S. Holloway, and D. L. Bartels, 2006: A multiwinter analysis of channeled flow through a prominent gap along the Northern California coast during CALJET and PACJET. *Mon. Wea. Rev.*, **134**, 1815–1841, https://doi.org/10.1175/MWR3148.1.

——, ——, G. A. Wick, J. D. Lundquist, and M. D. Dettinger, 2008: Meteorological characteristics and overland precipitation impacts of atmospheric rivers affecting the west coast of North America based on eight years of SSM/I satellite observations. *J. Hydrometeor.*, **9**, 22–47, https://doi.org/10.1175/2007JHM855.1.

——, B. J. Moore, A. B. White, G. A. Wick, J. Aikins, D. L. Jackson, J. R. Spackman, and F. M. Ralph, 2016: An airborne and ground-based study of a long-lived and intense atmospheric river with mesoscale frontal waves impacting California during CalWater-2014. *Mon. Wea. Rev.*, **144**, 1115–1144, https://doi.org/10.1175/MWR-D-15-0319.1.

NOAA, 2019a: Physical Science Division wind profiler data. Earth System Research Laboratory, accessed 22 April 2019, www.esrl.noaa.gov/psd/data/obs/datadisplay/.

——, 2019b: NOAA's habitat blueprint. Accessed 22 April 2019, www.habitatblueprint.noaa.gov/.

——, 2019c: NOAA's habitat focus areas. Accessed 22 April 2019, www.habitatblueprint.noaa.gov/habitat-focus-areas/.

Oakley, N. S., J. T. Lancaster, M. L. Kaplan, and F. M. Ralph, 2017: Synoptic conditions associated with cool season post-fire debris flows in the Transverse Ranges of Southern California. *Nat. Hazards*, **88**, 327–354, https://doi.org/10.1007/S11069-017-2867-6.

Ortega, J. A., L. Razola, and G. Garzón, 2014: Recent human impacts and change in dynamics and morphology of ephemeral rivers. *Nat. Hazards Earth Syst. Sci.*, **14**, 713–730, https://doi.org/10.5194/nhess-14-713-2014.

Potter Valley Project, 2020: Overview. Accessed 30 April 2020, http://pottervalleyproject.org/overview/.

PRISM Climate Group, 2019: PRISM climate data. Oregon State University, accessed 28 November 2018, http://prism.oregonstate.edu.

Ralph, F. M., and M. D. Dettinger, 2011: Storms, floods, and the science of atmospheric rivers. *Eos, Trans. Amer. Geophys. Union*, **92**, 265–266, https://doi.org/10.1029/2011EO320001.

——, and ——, 2012: Historical and national perspectives on extreme West Coast precipitation associated with atmospheric rivers during December 2010. *Bull. Amer. Meteor. Soc.*, **93**, 783–790, https://doi.org/10.1175/BAMS-D-11-00188.1.

——, P. J. Neiman, D. E. Kingsmill, P. O. Persson, A. B. White, E. T. Strem, E. D. Andrews, and R. C. Antweiler, 2003: The impact of a prominent rain shadow on flooding in California's Santa Cruz mountains: A CALJET case study and sensitivity to the ENSO cycle. *J. Hydrometeor.*, **4**, 1243–1264, https://doi.org/10.1175/1525-7541(2003)004<1243:TIOAPR>2.0.CO;2.

——, ——, and G. A. Wick, 2004: Satellite and CALJET aircraft observations of atmospheric rivers over the eastern North Pacific Ocean during the winter of 1997/98. *Mon. Wea. Rev.*, **132**, 1721–1745, https://doi.org/10.1175/1520-0493(2004)132<1721:SACAOO>2.0.CO;2.

——, and Coauthors, 2005a: Improving short-term (0–48 h) cool-season quantitative precipitation forecasting: Recommendations from a USWRP workshop. *Bull. Amer. Meteor. Soc.*, **86**, 1619–1632, https://doi.org/10.1175/BAMS-86-11-1615.

——, P. J. Neiman, and R. Rotunno, 2005b: Dropsonde observations in low-level jets over the northeastern Pacific Ocean from CALJET-1998 and PACJET-2001: Mean vertical-profile and atmospheric-river characteristics. *Mon. Wea. Rev.*, **133**, 889–910, https://doi.org/10.1175/MWR2896.1.

——, ——, G. A. Wick, S. I. Gutman, M. D. Dettinger, D. R. Cayan, and A. B. White, 2006: Flooding on California's Russian River: Role of atmospheric rivers. *Geophys. Res. Lett.*, **33**, L13801, https://doi.org/10.1029/2006GL026689.

——, E. Sukovich, D. Reynolds, M. Dettinger, S. Weagle, W. Clark, and P. J. Neiman, 2010: Assessment of extreme quantitative precipitation forecasts and development of

regional extreme event thresholds using data from HMT-2006 and COOP observers. *J. Hydrometeor.*, **11**, 1286–1304, https://doi.org/10.1175/2010JHM1232.1.

——, T. Coleman, P. J. Neiman, R. J. Zamora, and M. D. Dettinger, 2013a: Observed impacts of duration and seasonality of atmospheric-river landfalls on soil moisture and runoff in coastal Northern California. *J. Hydrometeor.*, **14**, 443–459, https://doi.org/10.1175/JHM-D-12-076.1.

——, and Coauthors, 2013b: The emergence of weather-related test beds linking research and forecasting operations. *Bull. Amer. Meteor. Soc.*, **94**, 1187–1211, https://doi.org/10.1175/BAMS-D-12-00080.1.

——, and Coauthors, 2014: A vision for future observations for western U.S. extreme precipitation and flooding. *J. Contemp. Water Res. Educ.*, **153**, 16–32, https://doi.org/10.1111/j.1936-704X.2014.03176.x.

——, and Coauthors, 2016a: The California Land-Falling Jets Experiment (CALJET): Objectives and design of a coastal atmosphere–ocean observing system deployed during a strong El Niño. *Third Symp. on Integrated Observing Systems*, Dallas, TX, Amer. Meteor. Soc., 8.1, https://ams.confex.com/ams/older/99annual/abstracts/1737.htm.

——, and Coauthors, 2016b: CalWater field studies designed to quantify the roles of atmospheric rivers and aerosols in modulating U.S. West Coast precipitation in a changing climate. *Bull. Amer. Meteor. Soc.*, **97**, 1209–1228, https://doi.org/10.1175/BAMS-D-14-00043.1.

——, and Coauthors, 2017: Atmospheric rivers emerge as a global science and applications focus. *Bull. Amer. Meteor. Soc.*, **98**, 1969–1973, https://doi.org/10.1175/BAMS-D-16-0262.1.

——, and Coauthors, 2019a: ARTMIP-early start comparison of atmospheric river detection tools: How many atmospheric rivers hit Northern California's Russian River watershed? *Climate Dyn.*, **52**, 4973–4994, https://doi.org/10.1007/s00382-018-4427-5.

——, J. J. Rutz, J. M. Cordeira, M. Dettinger, M. Anderson, D. Reynolds, L. J. Schick, and C. Smallcomb, 2019b: A scale to characterize the strength and impacts of atmospheric rivers. *Bull. Amer. Meteor. Soc.*, **100**, 269–289, https://doi.org/10.1175/BAMS-D-18-0023.1.

Ren, D., R. Fu, L. M. Leslie, and R. E. Dickinson, 2011: Modeling the mudslide aftermath of the 2007 Southern California wildfires. *Nat. Hazards*, **57**, 327–343, https://doi.org/10.1007/s11069-010-9615-5.

Reynolds, D. W., T. Colman, D. J. Gottas, and T. LeFebvre, 2016: Utilization of real-time vineyard observations to produce downscaled temperature forecasts for frost protection operations. *J. Oper. Meteor.*, **4**, 1–21, https://doi.org/10.15191/nwajom.2016.0401.

Sloto, R. A., and M. Y. Crouse, 1996: HYSEP: A computer program for streamflow hydrograph separation and analysis. U.S. Geological Survey Water-Resources Investigations Rep. 96-4040, 46 pp.

Sonoma Water, 2018a: Water supply. Accessed 22 April 2019, www.sonomawater.org/water-supply/.

——, 2018b: Current water supply levels. Accessed 2 May 2019, www.sonomawater.org/current-water-supply-levels.

——, 2019: Sonoma county real-time rainfall, river-stream, and reservoir data. Accessed 22 April 2019, https://sonoma.onerain.com/home.php.

State Water Resources Control Board, 1986: Russian River Project Application 19351 and petitions on Permits 12947A, 12949, 12950, and 16596 issued on applications 12919A, 15736, 15737; and 19351 of Sonoma County Water Agency East Fork Russian River, Russian River, and in Mendocino and Sonoma Counties Dry Creek. State Water Resources Control Board Decision 1610, 70 pp., www.waterboards.ca.gov/waterrights/board_decisions/adopted_orders/decisions/d1600_d1649/wrd1610.pdf.

Stohl, A., C. Forster, and H. Sodemann, 2008: Remote sources of water vapor forming precipitation on the Norwegian west coast at 60°N—A tale of hurricanes and an atmospheric river. *J. Geophys. Res.*, **113**, D05102, https://doi.org/10.1029/2007JD009006.

Sukovich, E. M., F. M. Ralph, F. E. Barthold, D. W. Reynolds, and D. R. Novak, 2014: Extreme quantitative precipitation forecast performance at the Weather Prediction Center from 2001 to 2011. *Wea. Forecasting*, **29**, 894–911, https://doi.org/10.1175/WAF-D-13-00061.1.

Sumargo, E., and Coauthors, 2020: Additional RHONET dataset. HydroShare, accessed 29 January 2020, www.hydroshare.org/resource/3c3a2f3d491c4e4aa4ccb6764806eb8a.

Talbot, C. A., M. Ralph, and J. Jasperse, 2019: Forecast-informed reservoir operations: Lessons learned from a multi-agency joint research and operations effort. *Federal Interagency Sedimentation and Hydrologic Modeling Conf.*, Reno, Nevada, SEDHYD, www.sedhyd.org/2019/openconf/modules/request.php?module=oc_proceedings&action=view.php&id=320&file=1/320.pdf&a=Accept.

USACE, 2018: Major planned deviation to the Coyote Valley Dam-Lake Mendocino water control manual draft environmental assessment. Sonoma County Water Agency Rep., 105 pp., www.spn.usace.army.mil/Portals/68/docs/Environmental/LakeMendocinoMajorDeviationRequest_Draft%20EA.pdf?ver=2018-06-29-152652-583.

——, 2020: HEC-ResSim. Accessed 23 January 2020, hec.usace.army.mil/software/hec-ressim/.

USGS, 2019: USGS water data for the nation. Accessed 22 April 2019, https://waterdata.usgs.gov/nwis.

White, A. B., J. R. Jordan, B. E. Martner, F. M. Ralph, and B. W. Bartram, 2000: Extending the dynamic range of an S-band radar for cloud and precipitation studies. *J. Atmos. Oceanic Technol.*, **17**, 1226–1234, https://doi.org/10.1175/1520-0426(2000)017<1226:ETDROA>2.0.CO;2.

——, D. J. Gottas, E. Strem, F. M. Ralph, and P. J. Neiman, 2002: An automated brightband height detection algorithm for use with Doppler radar spectral moments. *J. Atmos. Oceanic Technol.*, **19**, 687–697, https://doi.org/10.1175/1520-0426(2002)019<0687:AABHDA>2.0.CO;2.

——, P. J. Neiman, F. M. Ralph, D. E. Kingsmill, and P. O. Persson, 2003: Coastal orographic rainfall processes observed by radar during the California Land-Falling Jets Experiment. *J. Hydrometeor.*, **4**, 264–282, https://doi.org/10.1175/1525-7541(2003)4<264:CORPOB>2.0.CO;2.

——, and Coauthors, 2013: A twenty-first-century California observing network for monitoring extreme weather events. *J. Atmos. Oceanic Technol.*, **30**, 1585–1603, https://doi.org/10.1175/JTECH-D-12-00217.1.

——, P. J. Neiman, J. M. Creamean, T. Coleman, F. M. Ralph, and K. A. Prather, 2015: The impacts of California's San Francisco Bay Area gap on precipitation observed in the Sierra Nevada during HMT and CalWater. *J. Hydrometeor.*, **16**, 1048–1069, https://doi.org/10.1175/JHM-D-14-0160.1.

Willie, D., H. Chen, V. Chandrasekar, and R. Cifelli, 2017: Evaluation of multisensory quantitative precipitation estimation in Russian River basin. *J. Hydrol. Eng.*, **22**, E5016002 https://doi.org/10.1061/(ASCE)HE.1943-5584.0001422.

Wilson, A. M., and Coauthors, 2019: Training the next generation of researchers in the science and application of atmospheric rivers. *Bull. Amer. Meteor. Soc.*, **101**, E738–E743, https://doi.org/10.1175/BAMS-D-19-0311.1.

Yu, Z., 2000: Assessing the response of subgrid hydrologic processes to atmospheric forcing with a hydrologic model system. *Global Planet. Change*, **25**, 1–17, https://doi.org/10.1016/S0921-8181(00)00018-7.

——, and Coauthors, 1999: Simulating the river-basin response to atmospheric forcing by linking a mesoscale meteorological model and hydrologic model system. *J. Hydrol.*, **218**, 72–91, https://doi.org/10.1016/S0022-1694(99)00022-0.

Yuba Water Agency, 2020: Forecast-coordinated operations. Accessed 23 January 2020, www.yubawater.org/162/Forecast-Coordinated-Operations.

Zamora, R. J., F. M. Ralph, E. Clark, and T. Schneider, 2011: The NOAA Hydrometeorology Testbed soil moisture observing networks: Design, instrumentation, and preliminary results. *J. Atmos. Oceanic Technol.*, **28**, 1129–1140, https://doi.org/10.1175/2010JTECHA1465.1.

——, E. P. Clark, E. Rogers, M. B. Ek, and T. M. Lahmers, 2014: An examination of meteorological and soil moisture conditions in the Babocomari River basin before the flood event of 2008. *J. Hydrometeor.*, **15**, 243–260, https://doi.org/10.1175/JHM-D-12-0142.1.

Zhang, J., Y. Qi, D. Kingsmill, and K. Howard, 2012: Radar-based quantitative precipitation estimation for the cool season in complex terrain: Case studies from the NOAA Hydrometeorology Testbed. *J. Hydrometeor.*, **13**, 1836–1854, https://doi.org/10.1175/JHM-D-11-0145.1.